Volume 11 | Number 24 | 21 December 2024

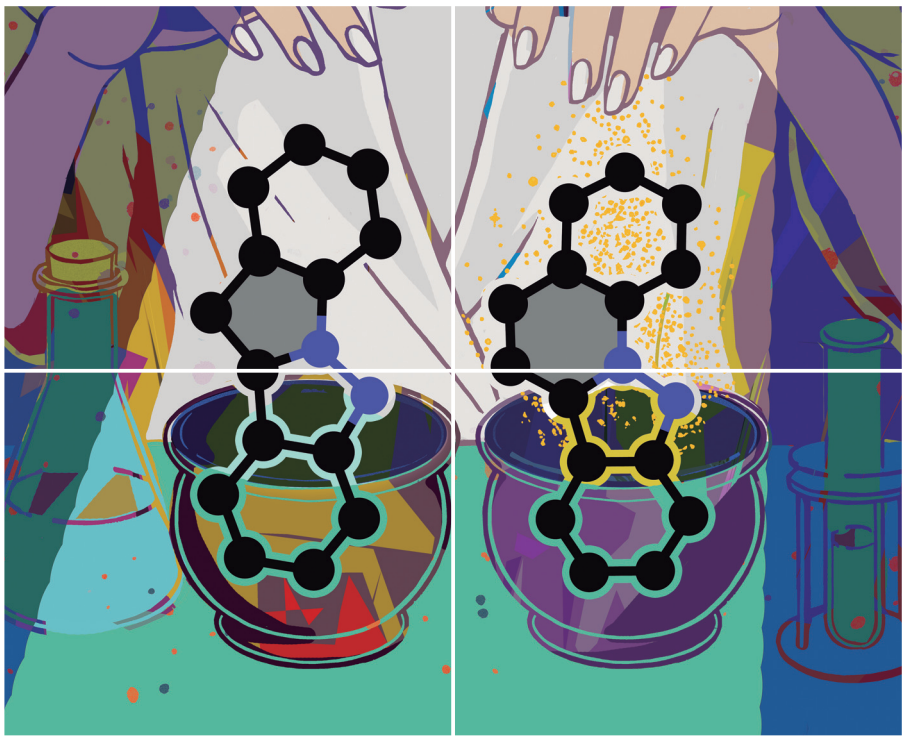

ORGANIC CHEMISTRY

FRONTIERS

CCS 中国化学会 CHINESE CHEMICAL SOCIETY

SIOC 1950

ROYAL SOCIETY OF CHEMISTRY

rsc.li/frontiers-organic

ORGANIC CHEMISTRY FRONTIERS

RESEARCH ARTICLE

View Article Online
View Journal | View Issue

Cite this: *Org. Chem. Front.*, 2024, **11**, 6974

Shaping cycles with light: a regiodivergent approach to tetracyclic aza-aromatic compounds†

Clara Mañas, [a,b] Belén Ibarra [a,b] and Estíbaliz Merino *[a,b]

Received 29th August 2024,
Accepted 7th October 2024

DOI: 10.1039/d4qo01606h

rsc.li/frontiers-organic

The development of regiodivergent methods that allow access to different structures from a single substrate through intramolecular processes is crucial for accelerating new molecule discovery, as well as making processes more sustainable and efficient in terms of waste production and economy. In this study, we report a novel regiodivergent cyclization procedure to access two distinct azapolyaromatic regioisomers from 2-alkynylazobenzenes. The key to achieving this regiodivergence lies in the presence or absence of a gold catalyst. The irradiation with visible light of 2-alkynylazobenzenes in the presence of a Ir photocatalyst affords 11*H*-indolo[1,2-*b*]indazoles, whereas under similar conditions with $AuCl_3$, indazolo[2,3-*a*]quinolines are produced. Control experiments and DFT calculations suggest that both transformations operate through different reaction mechanisms: the formation of 11*H*-indolo[1,2-*b*]indazoles involves a radical mechanism, whereas the formation of indazolo[2,3-*a*]quinolines appears to proceed predominantly through a polar mechanism. This transformation enables the one-step conversion of simple 2-alkynylazobenzenes into diverse azapolyaromatic structures *via* an intramolecular visible light-promoted process, holding significant potential for new nitrogenated heterocycles.

Introduction

Regiodivergent reactions represent a significant advancement in organic chemistry, offering the ability to produce different regioisomeric products from a single substrate under varying conditions. This versatility not only enhances the efficiency of synthetic routes by minimizing the need for multiple starting materials but also contributes to the sustainability of chemical processes by reducing waste and energy consumption. The ability to selectively access different structural isomers expands the chemical space available for new molecule discovery, facilitating the development of novel compounds with potential applications in pharmaceuticals, materials science, and agrochemicals. Thus, the development and understanding of regiodivergent reactions are crucial for advancing both the practical and theoretical aspects of modern organic synthesis.

Fused polycyclic (hetero)aromatic scaffolds are an essential class of compounds in organic chemistry characterized by their complex and rigid structures. These scaffolds are highly valued for their unique electronic properties serving as core structures in a wide range of functional materials, including organic semiconductors,[1] dyes,[2] and light-emitting diodes[3] and in a wide range of biologically active compounds,[4] so that the exploration and synthesis of these scaffolds continue to drive innovation in both materials science and drug discovery, highlighting their broad applicability and importance.

11*H*-Indolo[1,2-*b*]indazoles and indazolo[2,3-*a*]quinolines are two distinct classes of azapolyaromatic compounds with unique structural properties and potential applications. Indolo[1,2-*b*]indazoles are potent inhibitors of DNA topoisomerases I and II[5] but have been relatively unexplored. In contrast, indazoloquinolines, with their extended conjugated system, are used in fluorescence materials, such as OLED devices,[6] or as photocatalysts.[7] Quinolines are prevalent scaffolds in pharmacology, found in over 600 natural products, mainly alkaloids.[8] Both natural and synthetic quinolines exhibit a wide range of biological activities, including antifungal, antibacterial, antioxidant, anticancer, and antimalarial properties.[9] Despite their medicinal relevance and extensive investigation,[10] the fusion of quinolines with the indazole core to obtain indazolo[2,3-*a*]quinolines has been scarcely reported.

[a]*Universidad de Alcalá, Departamento de Química Orgánica y Química Inorgánica, Instituto de Investigación Andrés M. del Río (IQAR), Facultad de Farmacia, Alcalá de Henares, 28805 Madrid, Spain. E-mail: estibaliz.merino@uah.es*
[b]*Instituto Ramón y Cajal de Investigación Sanitaria (IRYCIS), Ctra. de Colmenar Viejo, Km. 9.100, 28034 Madrid, Spain*

† Electronic supplementary information (ESI) available. CCDC 2374941–2374943. For ESI and crystallographic data in CIF or other electronic format see DOI: https://doi.org/10.1039/d4qo01606h

Indolo[1,2-*b*]indazoles were first synthesized serendipitously by Wilshire in 1973[11] and later explored for their reactivity and bioactivity.[12] Various methodologies, including palladium and copper-catalyzed intramolecular C–N bond formation[13] at high temperatures and Rh(III)-catalyzed dehydrogenative annulation,[14] have been developed to synthesize these compounds. Additionally, the synthesis of these compounds can be achieved through a 1,4-dilithio intermediate formed by reacting 2-phenyl-2*H*-indazole with *n*-BuLi and trapping it with an acyl chloride.[15] Initially, indazolo[2,3-*a*]quinolines were synthesized in 1980 by Zurawel and Mitsuo.[16] These compounds have been explored through various methodologies, including PPh_3-mediated reductive cyclizations of 2-(*o*-nitrophenyl)quinolines,[17] aryne [3 + 2] dipolar cycloadditions,[18] the Pd-catalyzed tandem cross-coupling of 2-(*o*-iodophenyl)-2*H*-indazoles with organozinc reagents[19] as well as Rh(III)-catalyzed regioselective C–H functionalization of 2-aryl-2*H*-indazoles with alkynes,[20] α-diazo carbonyl compounds,[21] cyclic enones[22] or β-ketosulfoxonium ylides.[23] Additionally, rhodium-catalyzed cyclizations of azobenzenes[24] and 2-phenyl-2*H*-indazoles[25] with vinylene carbonate *via* C–H bond activation have also been reported (Fig. 1a). These efforts have expanded the scope and synthetic accessibility of indazolo[2,3-*a*]quinolines, allowing for the exploration of new applications for these compounds. Dihydroindazolo[2,3-*a*]quinolines can be synthesized *via* the Povarov reaction and a tandem process involving visible light-promoted intramolecular N–N bond formation using choline chloride/CuCl[26] or ruthenium complex (Fig. 1a).[27]

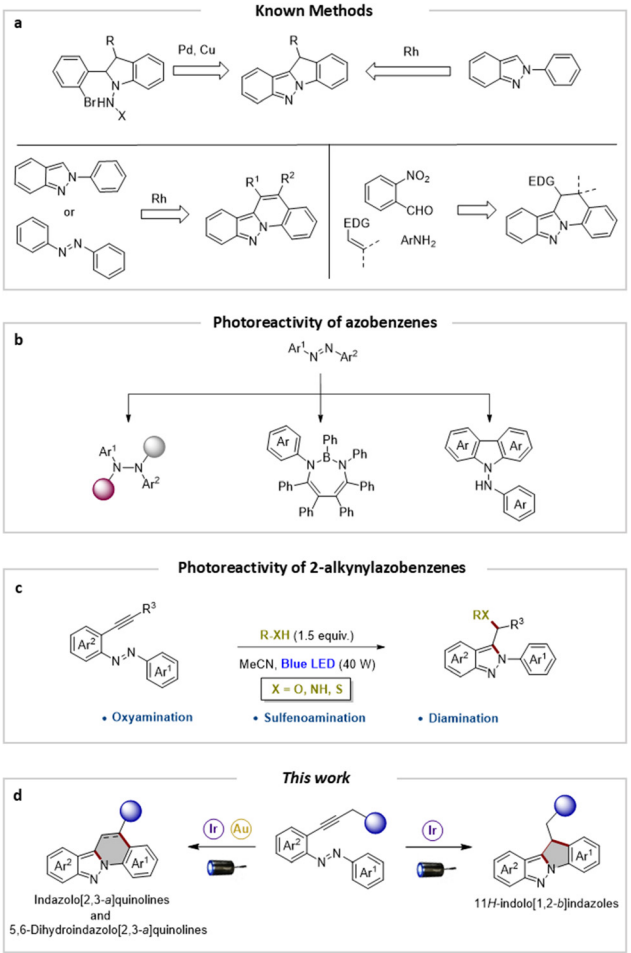

Fig. 1 (a) Approaches to synthesize 11*H*-indolo[1,2-*b*]indazoles, indazolo[2,3-*a*]quinolines and 5,6-dihydroindazolo[2,3-*a*]quinolines. (b) Photoreactivity of azobenzenes. (c) Photoreactivity of 2-alkynylazobenzenes. (d) Visible light-mediated regiodivergent synthesis of 11*H*-indolo[1,2-*b*]indazoles, indazolo[2,3-*a*]quinolines and 5,6-dihydroindazolo[2,3-*a*]quinolines from 2-alkynylazobenzenes.

Azobenzenes are ubiquitous molecules that play a central role in both fundamental and applied science. Initially investigated as dyes[28] their applications have expanded significantly into fields such as medicine, textiles, food, cosmetics as well as chemical sensing, organic transistors, and cell signaling.[29] Nowadays, research on azobenzenes is primarily centered on their *trans–cis* photoisomerization and remarkable photostability.[30,31] However, despite the growing interest in their photoisomerization properties, their application as synthetic intermediates in photo-induced reactions to form complex molecules remains underexplored. Since the 1960s, few examples have shown azobenzenes irradiated with UV or visible light to transform their scaffold. Most involve difunctionalization of the N=N bond without forming nitrogen-containing heterocycles.[32] A few examples involve forming complex molecules as seven-membered 1,3,2-diazaborepin heterocycles[33] or carbazoles[34] (Fig. 1b).

These examples highlight the potential of azobenzene reactivity under visible light irradiation for synthesizing nitrogen-containing heterocycles. Recently, our group reported a study on the heterodifunctionalization of 2-alkynylazobenzenes exclusively promoted by visible light, without the use of any transition metals or photocatalysts, describing oxyamination, sulfenoamination and diamination reactions (Fig. 1c).[35] This process exhibited excellent regioselectivity across a broad range of substrates and was characterized by its broad scope, simple set up, and mild reaction conditions.

We hypothesized that 2-alkynylazobenzenes could be engaged in additional bond-forming events in the presence of metal transitions and/or photocatalysts, thereby expanding the synthetic utility of these visible light-promoted processes. Consequently, we aimed to design cascade reactions that would enable the highly controlled synthesis of azapolyaromatic structures from 2-alkynylazobenzenes (Fig. 1d). First, we decided to test the reactivity of a 2-alkynylazobenzene **1a** by irradiating it with visible light in the presence of a photocatalyst. Our goal was to generate a reactive species of 2-alkynylazobenzene by the photocatalyst and visible light, to induce cyclization and form a 2*H*-indazole intermediate. This intermediate of radical nature could then undergo an additional cyclization with a phenyl ring through a subsequent C–C bond forming event.

Second, we speculated that the presence of a metal complex to activate the alkynyl moiety could lead to the formation of a 3-alkenyl-2*H*-indazole intermediate. This intermediate would then

evolve to form an additional C–C bond, generating a new ring of different size, as previously observed for similar compounds.[36]

Herein, we present the realization of these concepts through a regiodivergent strategy for synthesizing 11*H*-indolo[1,2-*b*]indazoles and indazolo[2,3-*a*]quinolines from 2-alkynylazobenzenes *via* intramolecular processes under photoredox conditions (Fig. 1d). To elucidate the nature of the productive reaction intermediates involved in these transformations, we conducted control experiments, mechanistic probes, and DFT calculations, the results of which will be presented. Our mechanistic studies suggest that different pathways operate depending on the presence or absence of $AuCl_3$ in the reaction medium. The ability to selectively synthesize these scaffolds from a common precursor demonstrates the versatility of modern synthetic methods. This provides valuable tools for synthesizing complex scaffolds from simple starting materials and expanding the catalogue of sustainable methodologies for organic synthesis that utilize visible light to promote transformations.

Results and discussion

Initially, (*E*)-1-(2-(hex-1-yn-1-yl)phenyl)-2-phenyldiazene (**1a**) was selected as a benchmark substrate to explore its photoreactivity. We began our investigation by studying the reactivity of this substrate using 5 mol% of $AuCl_3$ and 2 mol% of Ir[dF(CF_3)ppy]$_2$(dtbpy)PF_6 in MeCN at room temperature, irradiated with a blue LED (40 W) (Scheme 1).

Under these conditions, a mixture of four cyclization products was obtained: alongside indolo[1,2-*b*]indazole **2a**, 5,6-dihydroindazolo[2,3-*a*]quinoline **3a**, indazolo[2,3-*a*]quinoline **4a** and 3-alkenyl-2*H*-indazole **5a** were formed. **2a**, **3a**, and **4a** result from the formation of a C–N bond and a C–C bond, generating two five-membered rings for **2a** and one five-membered ring and one six-membered ring for compounds **3a** and **4a** in a single reaction step. Considering this result, we decided to optimize the synthesis of compounds **2a**, **3a**, and **4a** to selectively obtain different azapolycycles from 2-alkynylazobenzenes.

Firstly, our focus shifted to optimizing the formation of compound **2a**. A control experiment conducted without the gold(III) catalyst resulted in **2a** being the major product, which was isolated by column chromatography with a 34% yield (Table 1, entry 1). Next, we investigated the effect of the photocatalyst by testing various organometallic and organic photocatalysts (Fig. 2). Among the Ir(III) organometallic photocatalysts,

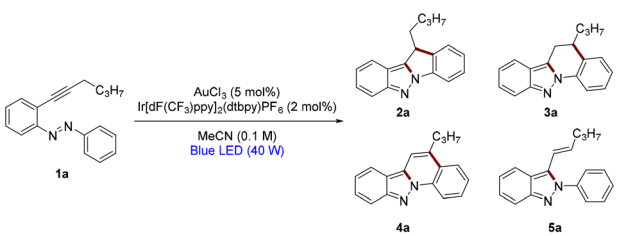

Scheme 1 Initial experiment.

Table 1 Optimization of reaction conditions for **2a**

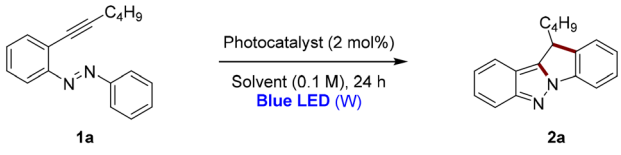

Entry	Blue LED (W)	Photocatalyst	Solvent	Yield[a] (%)
1	40	**PC1**	MeCN	34
2	40	**PC2**	MeCN	47
3	40	**PC3**	MeCN	62
4	40	**PC4**	MeCN	33
5	40	**PC5**	MeCN	15
6	40	**PC6**	MeCN	34
7	40	**PC7**	MeCN	24
8	40	**PC3**	Acetone	72
9	40	**PC3**	MeOH	0[b]
10	40	**PC3**	DCE	85
11	50	**PC3**	DCE	85
12	100	**PC3**	DCE	86

[a] Isolated yields after column chromatography on silica gel. [b] **A** was isolated with 90% yield.

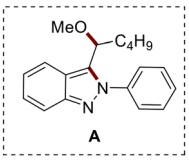

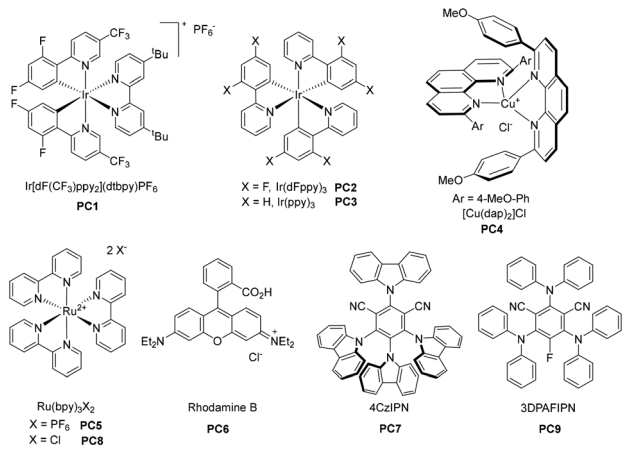

Fig. 2 Some of the photocatalysts tested in this work.

Ir(dFppy)$_3$ offered a yield of 47% (Table 1, entry 2), while Ir(ppy)$_3$ delivered a significantly improved yield of 62% (Table 1, entry 3). In contrast, photocatalysts derived from Cu(I) and Ru(II) resulted in lower yields (Table 1, entries 4 and 5). Organic photocatalysts from the xanthene family (Table S1†) as well as acridinium and 4CzIPN photocatalysts did not yield better results (Table 1, entries 6 and 7). Based on these findings, Ir(ppy)$_3$ was selected for further optimization studies. Regarding the solvents, acetone provided a better outcome than MeCN, yielding a 72% yield (Table 1, entry 8). Using

MeOH as a solvent favoured the formation of 3-(1-methoxypentyl)-2-phenyl-2*H*-indazole (**A**) with no indolo[1,2-*b*]indazole **2a** detected (Table 1, entry 9).[25] DCE emerged as the optimal solvent, achieving an 85% yield (Table 1, entry 10). Finally, the reaction was performed under irradiation with 50 or 100 W (Table 1, entries 11 and 12). No significant changes in the reaction were observed at 50 W and increasing the intensity to 100 W did not improve the yield or affect the reaction time.

With the optimized reaction conditions in hand, a scale-up experiment was conducted, increasing the scale tenfold (1 mmol) with compound **1a**. The corresponding product **2a** was isolated with a similar yield after purification by column chromatography (Scheme 2).

To demonstrate the versatility and robustness of our method for synthesizing indolo[1,2-*b*]indazoles **2** *via* C–N and C–C bond formation from 2-alkynylazobenzenes **1**, we set out to explore the substrate scope. A series of 2-alkynylazobenzenes **1**, with different modifications on both aromatic rings and the alkynyl chain, were subjected to the optimized reaction conditions. The method achieved moderate to very good yields across a broad range of functional groups, with

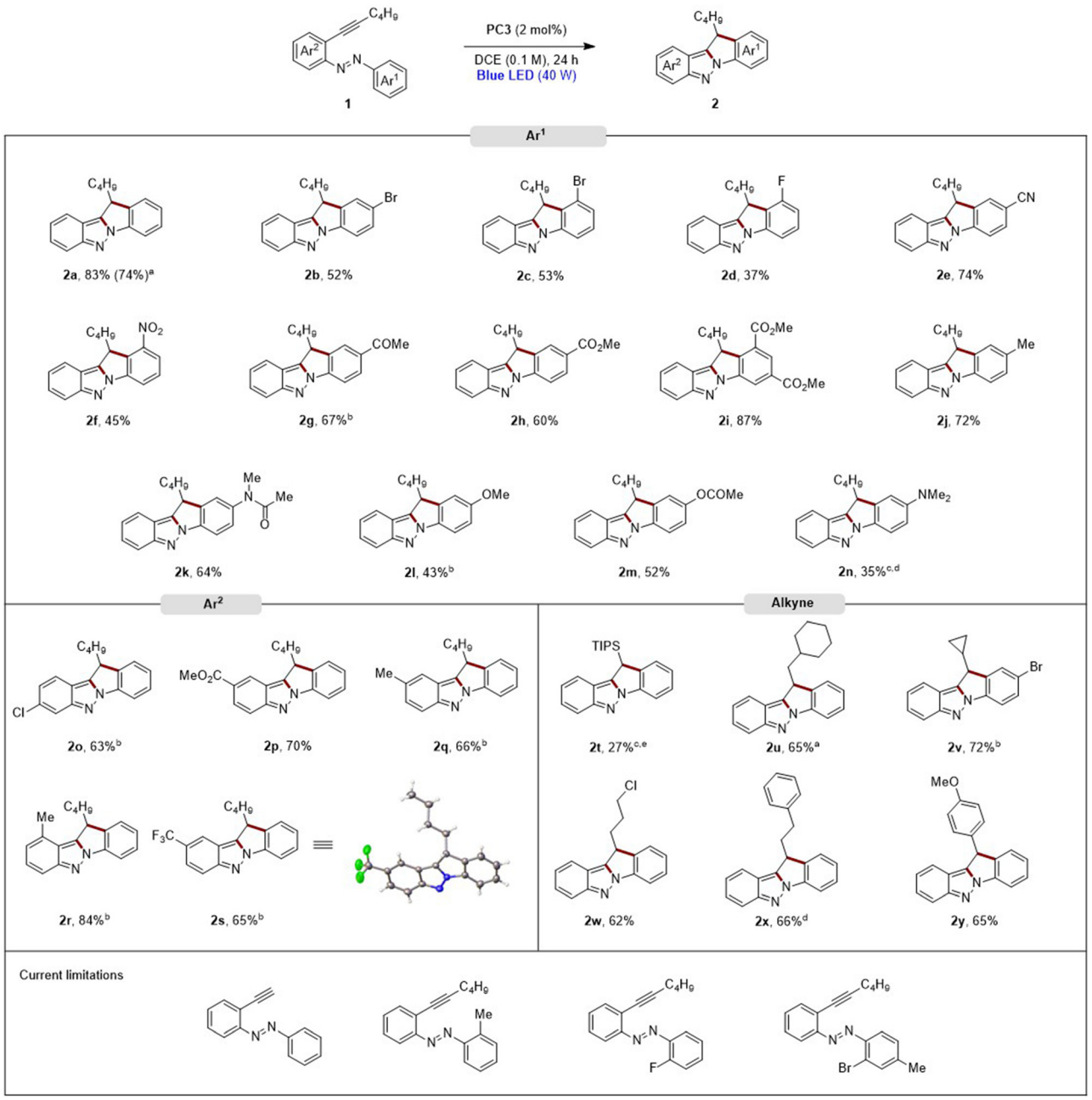

Scheme 2 Scope for the reaction from 2-alkynylazobenzenes **1** to indolo[1,2-*b*]indazoles **2**. [a] Reaction was carried out at 1 mmol scale. [b] Reaction time: 48 h. [c] Yield based on recovered starting material. [d] Reaction time: 72 h. [e] Reaction time: 7 days.

substitutions on both the *para* and the *meta* positions of Ar^1 being well tolerated (Scheme 2). Different halogen atoms were introduced at these positions, resulting in moderate yields (**2b–2d**). For **2c** and **2d**, the formation of the C–C bond exclusively occurred at the position of the aromatic ring with the azo group and halogen in the *ortho* position. Nitrogenated electron-withdrawing groups were successfully incorporated: a cyano group in the *para* position yielded **2e** with a 74%, and a nitro group in the *meta* position gave **2f** with 45% yield. Carbonylated electron-withdrawing groups such as ketones and esters (**2g** and **2h**), were introduced in the *para* position with good yields. A disubstituted substrate with ester groups delivered **2i** with a very good yield. Electron-donating groups were also evaluated: a methyl group at the *para* position produced **2j** successfully while an amide group led to a 64% yield of **2k**. Strong and weak oxygenated electron-donating groups gave moderate yields for **2l** and **2m**, with lower yields generally due to the formation of byproducts **3a** and **4a**. Nitrogenated electron-donating groups at the *para* position were also tested, but the reaction with a dimethylamino group did not achieve complete conversion after 7 days, yielding **2n** with a 35% yield. Further testing on the aromatic ring Ar^2 and the alkynyl chain showed good results. A chlorine atom at position 8 yielded **2o** with a 63% and an ester group at position 9 yielded **2p** with a 70% yield. Methyl groups at positions 9 and 10 resulted in good and very good yields, respectively (**2q** and **2r**), although with longer reaction times (48 hours). A trifluoromethyl group at position 9 gave **2s** with a 65% yield and the structure was confirmed by X-ray diffraction.[37] With a bulky protecting group as triisopropylsilyl group on the triple bond, the reaction achieved 70% conversion after 7 days isolating **2t** with 27% yield. Deprotection of the triisopropylsilyl ether group with TBAF and subsequent cyclization under standard conditions led to decomposition, likely due to the low stability of (*E*)-1-(2-ethynylphenyl)-2-phenyldiazene and the extended reaction time. Introducing cycloalkyl groups, a cyclohexyl group (**2u**) yielded 65%, while a cyclopropyl group (**2v**) gave a 72% yield. A chlorine atom in the alkynyl chain was compatible, providing **2w** with a 62% yield. Incorporating a phenyl group into the alkynyl chain or a *p*-methoxyphenyl group directly linked at the triple bond gave the corresponding products **2x** and **2y**, respectively, in similar good yields. With substrates containing substitutions in the *ortho* position of Ar^1 with fluorine, bromo or methyl groups, the corresponding indolo[1,2-*b*]indazoles **2** were not obtained, instead starting material, decomposition and dehalogenation products were recovered.

To investigate the mechanism of this reaction, experiments were designed to produce **2a** by deviating from standard conditions. When the reaction was carried out without a catalyst, a 33% yield of the product was observed. The role of light during the process was also evaluated. In the absence of light, the formation of **2a** was not observed, indicating its crucial role in this transformation. The reaction proceeds exclusively under light irradiation (Fig. 3a). Next, the reaction was conducted in the presence of a radical quencher. Using 2,6-di-*tert*-butyl-4-methylphenol (BHT), the resulting radical intermediate formed after the C–N bond formation was trapped, and compound **6** was isolated with a 39% yield. This result indicates the likely involvement of radical species along the reaction pathway. When the reaction was carried out with (*E*)-1-(hex-1-yn-1-yl)-2-styrylbenzene, after 36 hours of irradiation, only isomerization of the double bond was observed, yielding a 1 : 3.5 *E* : *Z* ratio. This result suggests that the excitation of the azo group by the photocatalyst triggers the reaction (Fig. 3b).

Next, two deuteration experiments were conducted. In the first, the reaction was performed using deuterated dichloroethane to determine whether deuterium incorporation into the product occurred *via* hydrogen transfer from the solvent to the substrate (Fig. 3c). In this case, product **2a** was isolated with an 81% yield, and no deuterium incorporation was observed. Subsequently, (*E*)-1-[2-(hex-1-yn-1-yl)phenyl]-2-(phenyl-d_5)-diazene (**1a-*d*$_5$**) was synthesized, and under standard reaction conditions, the corresponding deuterated compound **2a-*d*$_5$** was formed with a 67% yield and 97% deuteration (Fig. 3d). This suggests that during the reaction, a hydrogen atom from the aromatic ring Ar^1 migrates to the five-membered ring.

Analysis of the reaction progress by ^{1}H NMR revealed that (*Z*)-**1a** is generated during the reaction. The reaction profile, monitored by nuclear magnetic resonance spectroscopy, indicates that a photo-stationary equilibrium of the *cis–trans* isomers of **1a** is reached at 10 minutes. The concentration of both isomers decreases during the reaction, while the product yield increases. After 7 hours, a 10% formation of indazole **5a** was observed (Fig. 3e).

To gain deeper insight into the mechanism operating in this transformation, DFT calculations were conducted (Fig. 3g). The initial step, the formation of the 2-phenyl-2*H*-indazole intermediate **II** from the radical cation **I** generated by activating **1a** with the Ir catalyst, is both kinetically and thermodynamically favorable ($\Delta G^{\ddagger}$ = +5.5 kcal mol^{-1} and ΔG = −5.3 kcal mol^{-1}). Subsequently, two distinct mechanistic pathways can be proposed. The first pathway involves cyclization to form the C–C bond, leading to intermediate **III**, followed by a 1,2-intramolecular hydrogen migration to furnish intermediate **IV**. The second pathway considers the 1,5-intramolecular hydrogen migration occurs before C–C bond formation. The formation of the C–C bond is favored by 6.3 kcal mol^{-1} over the 1,5-intramolecular hydrogen migration, making the first pathway more likely. The formation of intermediate **III** from **II** *via* C–C bond formation has a kinetic barrier of $\Delta G^{\ddagger}$ = +6.8 kcal mol^{-1} and is highly thermodynamically favored (ΔG = −22.8 kcal mol^{-1}). The subsequent 1,2-intramolecular hydrogen migration is the rate-determining step, with a kinetic barrier of $\Delta G^{\ddagger}$ = +12.4 kcal mol^{-1}.

Following the experimental and computational investigations above, we propose a plausible mechanism (Fig. 3f). The reaction likely begins with the activation of the Ir catalyst by visible light absorption, forming an excited Ir species. This

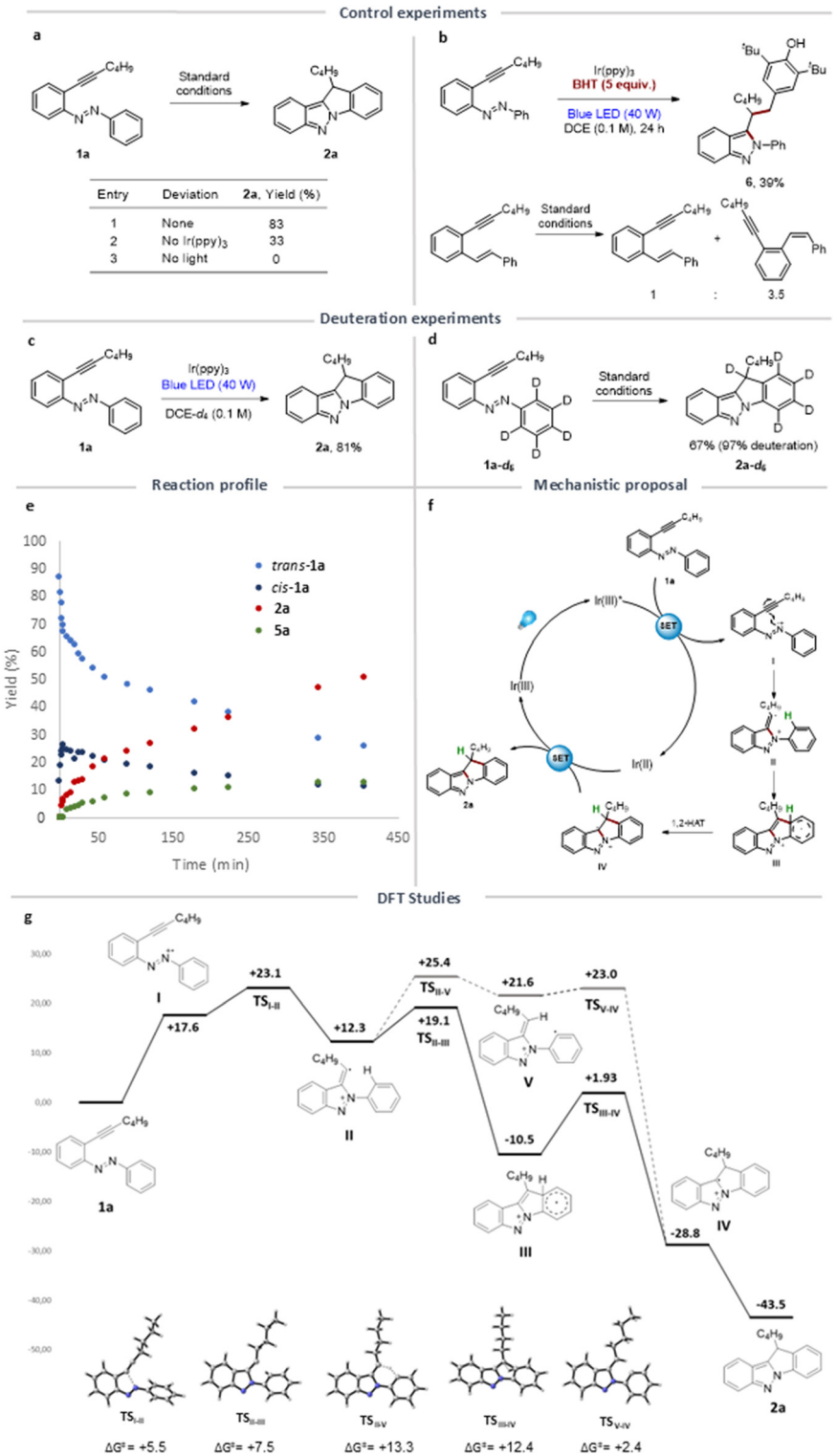

Fig. 3 (a) and (b) Control experiments. (c) and (d) Deuteration experiments. (e) Kinetic study. (f) Mechanistic proposal. (g) Computed reaction coordinate profile of the reaction to synthesize indolo[1,2-*b*]indazole **2a** from (*E*)-1-(2-(hex-1-yn-1-yl)phenyl)-2-phenyldiazene **1a**. All calculations were conducted at B3LYP/6-31g+(d,p)/IEFPCM (solvent = DCE) level of theory (see ESI† for full details). The energy values are given in kcal mol^{-1}.

is followed by a single-electron transfer (SET) process, where 2-alkynylazobenzene **1a** transfers an electron to the Ir catalyst, generating an Ir(II) species and a radical cation **I**. The C–N bond is then formed by the attack of a nitrogen atom on a carbon of the alkyne group, producing the radical cation **II** of the indazole intermediate. Next, the C–C bond formation

occurs to generate intermediate **III**, followed by a 1,2-hydrogen atom transfer. Finally, a second SET process closes the catalytic cycle, forming compound **2a**.

The next goal was to optimize the reaction conditions for obtaining indazolo[2,3-*a*]quinolines **4**. The benchmark substrate for optimization was again **1a**. An experiment was conducted using 2-alkynylazobenzene **1a** (0.2 mmol), with $AuCl_3$ (5 mol%) and $Ir[dF(CF_3)ppy]_2(dtbpy)PF_6$ (2 mol%) in MeCN (0.1 M), irradiated with blue light (40 W) for 24 hours (Table 2, entry 1). In this case, 2*H*-indazole **5a** was the main product with a 45% yield, while 5,6-dihydroindazolo[2,3-*a*]quinoline **3a** and indazolo[2,3-*a*]quinoline **4a** were minor products, yielding 20% and a 5%, respectively, as determined by ^1H NMR. Increasing the blue LED potency to 80 W (Table 2, entry 2) reduced the yield of 2*H*-indazole **5a** to 27% yield, with a corresponding increase in the yields of **3a** and **4a** to 29% and 10%, respectively. When the irradiation was further increased to 100 W, the temperature rose to 70 °C (Table 2, entry 3). Under these conditions, no 2*H*-indazole **5a** was observed. Instead, a 50% yield of 5,6-dihydroindazolo[2,3-*a*]quinoline **3a** and a 30% yield of indazolo[2,3-*a*]quinoline **4a** were detected by ^1H NMR. Next, different gold(III) catalysts were tested. $AuBr_3$ showed promising results, furnishing 49% yield of **3a** and 24% yield of **4a** (Table 2, entry 4). In contrast, $Au(OAc)_3$ was less effective, providing only a 29% yield of **3a** with negligible amounts of **4a** (Table 2, entry 5). A copper(I) catalyst, $Cu(MeCN)_4BF_4$ was also evaluated (Table 2, entry 6). Despite achieving a 17% yield of **4a**, the overall results did not show significant improvement. After testing several catalysts, no substantial improvements were observed.[38] Copper (**PC4**) and ruthenium (**PC8**) photocatalysts predominantly produced **5a** (Table 2, entries 7 and 8). In contrast, using 2DPAFIPN (**PC9**) shifted the major product to **3a** (Table 2, entry 9). Other solvents were tested, DCE yielded only 30% yield of **3a** and traces of **4a**, whereas acetone produced a mixture of **3a** and **4a** with yields of 15% and traces, respectively (Table 2, entries 10 and 11). Notably, no presence of **5a** was detected in both experiments.

Recognizing that both 3-alkenyl-2*H*-indazole **5a** and 5,6-dihydroindazolo[2,3-*a*]quinoline **3a** are likely intermediates, further experiments with extended reaction times or enhanced blue LED power were conducted. These conditions achieved complete conversion, with longer reaction times favouring the formation of indazolo[2,3-*a*]quinoline **4a**. However, increased reaction times also led to higher decomposition of the compounds. To improve the yield of **4a**, the addition of an oxidant was tested to oxidize 5,6-dihydroindazolo[2,3-*a*]quinoline **3a** into the corresponding indazolo[2,3-*a*]quinoline **4a**. (Diacetoxyiodo)benzene initially yielded exclusively **4a** but with low yield (Table 2, entry 12). Other oxidants as NBS, IBX, cyclooctene and MnO_2 were tested but no improvement in the yields of **4a** were obtained (Tables S3 and S4†). Given DDQ's effectiveness as an oxidant, we tried adding it after 24 hours of irradiation and filtering the mixture over silica. Although this resulted in complete oxidation to **4a**, the yield was only 32% yield and the formation of decomposition byproducts (Table 2, entry 13). To minimize decomposition and promote oxidation, we added only 1.2 equivalents of DDQ, used 1,4-dioxane as the solvent for the second reaction step, and reduced the blue LED irradiation to 80 W. Under these conditions, **4a** along with **3a** were isolated by column chromatography with a yield of 53% (Table 2, entry 14).

Instances of photocatalyzed dehydrogenations have been documented through distinct mechanisms, including the

Table 2 Optimization of reaction conditions for **4a**

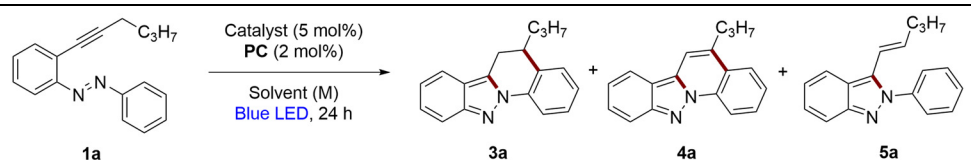

1a **3a** **4a** **5a**

Entry	Blue LED (W)	Catalyst	PC	Solvent	Oxidant (2 equiv.)	**3a**[a] (%)	**4a**[a] (%)	**5a**[a] (%)
1	40	$AuCl_3$	**PC1**	MeCN	—	20	5	45
2	80	$AuCl_3$	**PC1**	MeCN	—	29	10	27
3	100	$AuCl_3$	**PC1**	MeCN	—	50	30	—
4	100	$AuBr_3$	**PC1**	MeCN	—	49	24	—
5	100	$Au(OAc)_3$	**PC1**	MeCN	—	29	Traces	—
6	100	$Cu(MeCN)_4BF_4$	**PC1**	MeCN	—	38	17	—
7	100	$AuCl_3$	**PC4**	MeCN	—	—	—	35
8	100	$AuCl_3$	**PC8**	MeCN	—	25	Traces	48
9	100	$AuCl_3$	**PC9**	MeCN	—	38	5	—
10	100	$AuCl_3$	**PC1**	DCE	—	30	Traces	—
11	100	$AuCl_3$	**PC1**	Acetone	—	15	Traces	—
12	100	$AuCl_3$	**PC1**	MeCN	$PhI(OAc)_2$	0	18	—
13	100	$AuCl_3$	**PC1**	MeCN	DDQ	0	32	—
14[b,c]	100	$AuCl_3$	**PC1**	MeCN	DDQ	7	46	—

[a] Yields calculated by ^1H NMR, using dibromomethane as internal standard. [b] Reaction was performed in two steps: (i) $AuCl_3$ (5 mol%), $Ir[dF(CF_3)ppy_2](dtbpy)PF_6$ (2 mol%), MeCN (0.1 M), Blue LED (100 W), 70 °C, 24 h. (ii) DDQ (1.2 equiv.), 1,4-dioxane (0.1 M), Blue LED (80 W), 50 °C, 24 h. [c] Isolated yield (**3a** + **4a**) by column chromatography.

generation of hydrogen gas, which increases the pressure in the reaction vessel.[39] Our reaction conducted in a 5 mL pressure Schlenk, led to the hypothesis that the liberated H_2 increased the pressure, potentially slowing the reaction rate. To address this, we modified the set up. Initially, the reaction was carried out in a round-bottom flask with a balloon punctured through the septum, resulting in significant hydrazine formation, indicating decomposition of the starting material.

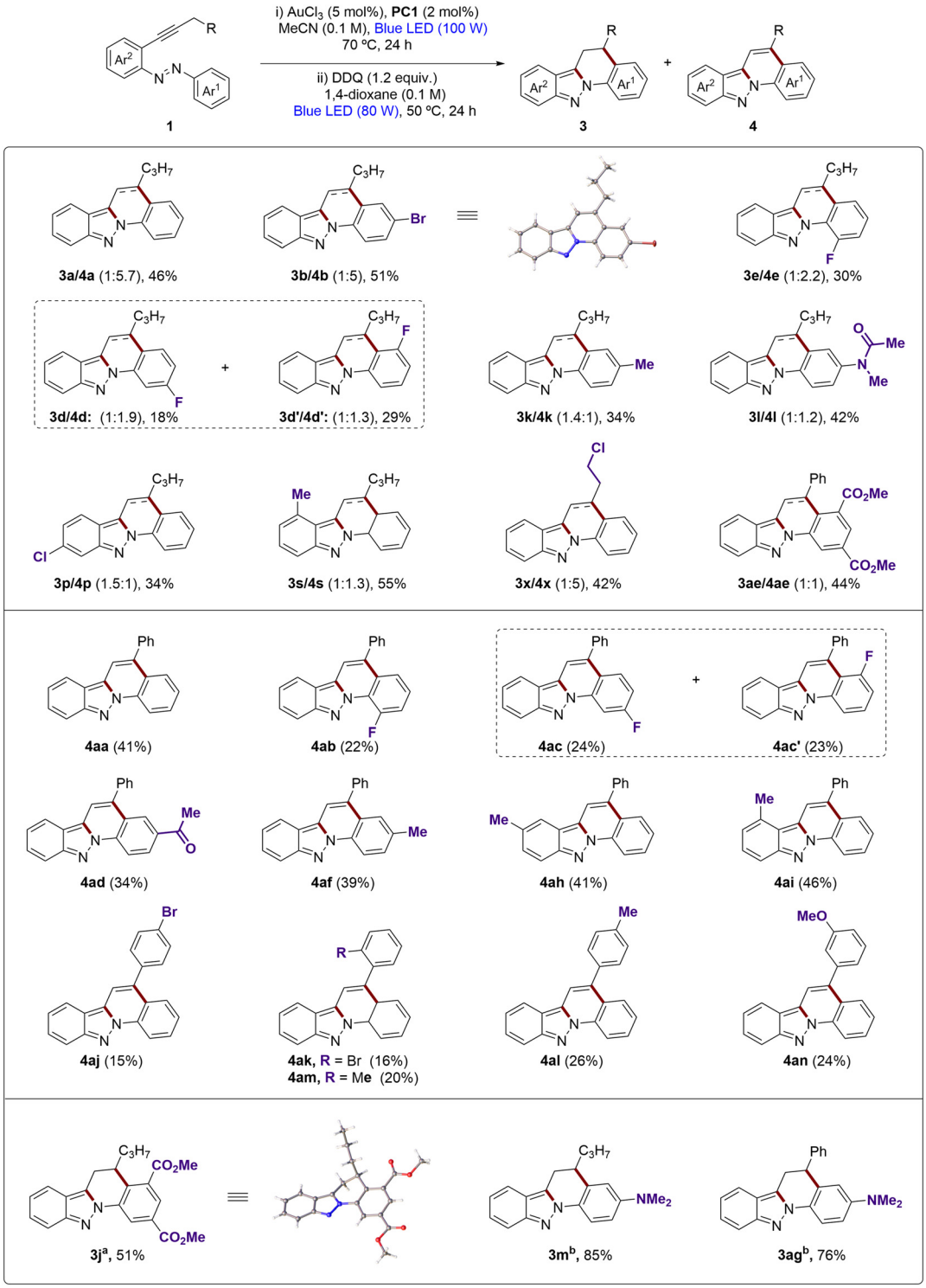

Scheme 3 Scope for the reaction from 2-alkynylazobenzenes **1** to 5,6-dihydroindazolo[2,3-*a*]quinolines **3** and indazolo[2,3-*a*]quinolines **4**. [a] Conditions: $AuCl_3$ (5 mol%), **PC1** (2 mol%), MeCN (0.1 M), Blue LED (30 W), 25 °C, 24 h. [b] Conditions: $AuCl_3$ (5 mol%), **PC1** (2 mol%), MeCN (0.1 M), Blue LED (100 W), 70 °C, 24 h.

Conducting the reaction in a Schlenk tube improved the outcome, yielding a 3 : 10 ratio of 5,6-dihydroindazolo[2,3-*a*]quinoline **3a** to indazolo[2,3-*a*]quinoline **4a**, but trace hydrazine still indicated ongoing decomposition. We then used a pressure Schlenk for the first 24 hours, ensuring full conversion of the starting material to **3a** and **4a**, followed by transferring the mixture under argon to a Schlenk tube for another 24 hours of irradiation. This afforded only indazolo[2,3-*a*]quinoline **4a**, but with a low ^{1}H NMR yield of 27%, suggesting further decomposition.[38] Finally, performing the entire reaction in a pressure Schlenk with periodic pressure releases resulted in a 5 : 4 ratio of **3a** and **4a**, indicating incomplete conversion. After optimizing the reaction conditions to obtain indazolo[2,3-*a*]quinoline **4a**, the scope of the reaction was explored (Scheme 3). A variety of 2-alkynylazobenzenes **1**, with modifications on the aromatic rings and alkynyl chain, were evaluated. The corresponding indazolo[2,3-*a*]quinolines **4** were obtained in synthetically useful yields. Products without substitution (**3a**/**4a**) or with halogens in Ar^1, such as bromine in the *para* position (**3b**/**4b**) or fluorine in the *ortho* position (**3e**/**4e**), were isolated with yields ranging from 30–51%. The structure of **4b** was confirmed by X-Ray diffraction.[37] When a fluorine atom was present in the *meta* position, a mixture of the 2- and 3-substituted products (**3d**/**4d** and **3d′**/**4d′**) was obtained with yields of 18 and 29%, respectively. Electron-donating groups were also assessed. A methyl group or *N*-methylacetamide gave the corresponding products in moderate yields (**3k**/**4k** and **3l**/**4l**). Modifications on the aromatic ring Ar^2 were also evaluated. Compounds with a chlorine atom in position 9 and a methyl group in position 7 were isolated with yields of 34 and 55%, respectively (**3p**/**4p** and **3s**/**4s**). Modifications to the alkynyl chain were also explored. 2-Alkynylazobenzene **1x**, with a chlorine atom at the end of the alkyl chain, delivered **3x**/**4x** with a 42% yield.[40] The introduction of an extra phenyl group directly conjugated with the indazolo[2,3-*a*]quinoline core enabled the exclusive isolation of the desired compound **4aa** with a 41% yield. Due to this result, we investigated the scope using a benzyl substituent on the alkynyl moiety. With a fluorine substituent on Ar^1 in the *ortho* position relative to the azo group, the tetracycle **4ab** could be isolated in pure form, albeit with a low yield. The substrate **1ac**, with the fluorine atom in the *meta* position relative to the azo group, under standard reaction conditions, led to a mixture of compounds **4ac** and **4ac′** with 24% and 23% yields, respectively. Substrates with acetyl or methyl substituents on Ar^1, or methyl groups in positions 7 and 8 on Ar^2, resulted in moderate yields of **4ad–4ai**. Given the exclusive selectivity for forming **4** with a benzyl substituent on the alkynyl fragment, we decided to study the variability of substituents on this aromatic ring. Substrates with electron-withdrawing groups like bromine and electron-donating groups like methyl and methoxy in different positions allowed the exclusive isolation of compounds **4aj–4an** with yields between 15% and 26%. Selective isolation of compound **3j** with a yield of 51% allowed confirmation of its structure by X-ray diffraction.[37] This example, along with substrate **1ae**, demonstrates that selective formation of **3** can be achieved by modifying the alkynyl fragment when the substrate presents two CO_2Me groups on Ar^1. Given these results, the synthesis of starting substrates with other electron-withdrawing groups in the *meta* position, such as nitro and bromo substituents was proposed to selectively obtain 5,6-dihydroindazolo[2,3-*a*]quinolines **3**. However, the synthesis of these substrates was not successful. Surprisingly, when the aromatic ring Ar^1 has a dimethylamino group, high yields of compounds **3m** and **3ag** were obtained regardless of whether the alkynyl fragment had an alkyl or aromatic group. The results from this scope study suggest that the reaction selectivity is strongly influenced by the electronic nature of the substituents.

To gain a deeper understanding of the reaction, experiments were designed to synthesize **4a** by deviating from standard conditions (Fig. 4a). When the reaction was performed without $AuCl_3$, the yield was 18% for **3a** and traces of **4a**, with 34% of the mixture identified as indolo[1,2-*b*]indazole **2a**. This outcome highlighted the lack of selectivity in the absence of gold(III). In a second experiment without the photocatalyst, the yield was 34% (**3a** + **4a**), with no other products detected. These results suggest that the yield decreases primarily during the formation of the 3-alkenyl-2*H*-indazole **5**, rather

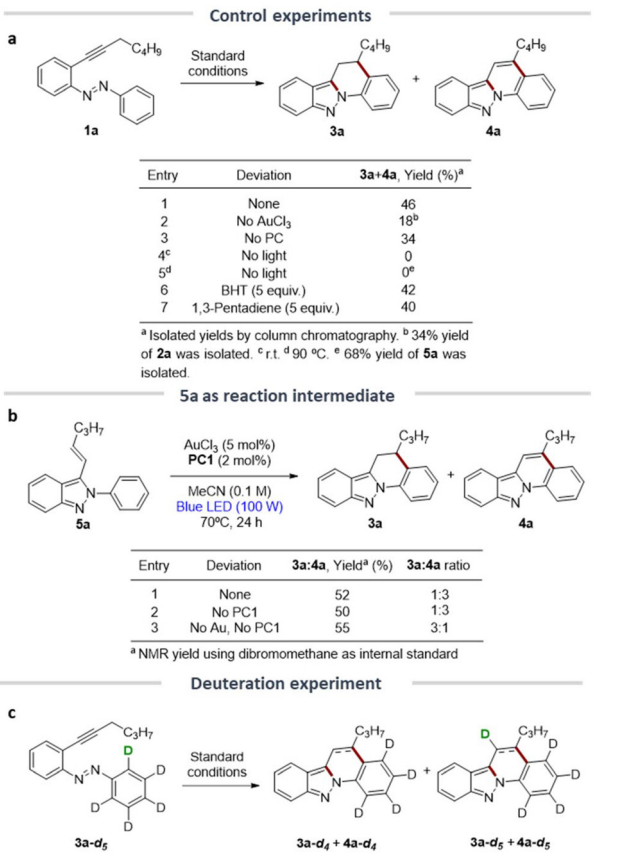

Fig. 4 (a) Control experiments. (b) Reactions with **5a**. (c) Deuteration experiment.

than during the subsequent C–C bond formation to generate the 5,6-dihydroindazolo[2,3-*a*]quinoline **3a**. When the reaction was carried out in the dark conditions at room temperature, no conversion to the desired product was observed. Similarly, a reaction conducted in the dark at 90 °C yielded no traces of **3a** or **4a** but resulted in a 68% yield of 3-alkenyl-2*H*-indazole **5a**. Next, a control experiment with a radical scavenger was performed by adding 5 equivalents of BHT to the standard reaction conditions for both steps. This resulted in a mixture of **3a** and **4a** in a 2.3 : 1 ratio with a 42% yield. A similar result was obtained when 1,3-pentadiene, a known triplet quencher, was used.[41] Notably, no traces of **1a** or **5a** were detected, confirming the involvement of a polar mechanism for the first part of the reaction. However, the ratio of **3a** to **4a** suggested that the oxidation from **3a** to **4a** might involve a radical pathway.

To prove that **5a** is an intermediate in the reaction pathway, 3-alkenyl-2*H*-indazole **5a** (0.02 mmol), $AuCl_3$ (5 mol%) and Ir[dF(CF$_3$)ppy]$_2$(dtbpy)PF$_6$ (2 mol%) were dissolved in MeCN and irradiated with a blue LED (100 W) for 24 hours. This produced a 52% yield of N-heterocycles **3a** and **4a**. In absence of **PC1**, the yield and the **3a** : **4a** ratio were similar to the previous experiment. Another reaction, without $AuCl_3$ and **PC1**, produced **3a** and **4a** with a 55% yield and a 3 : 1 ratio. These results support the assumption that both Au(III) and Ir(III) catalysts promote the formation of **5a** and that **5a** is likely an intermediate in the reaction (Fig. 4b). They also indicate that the intramolecular cyclization to form the six-membered ring is exclusively promoted by visible light.

To determine whether the hydrogen at position 6 in **4a** originated from the aromatic ring of **3a**, (*E*)-1-[2-(hex-1-yn-1-yl) phenyl]-2-(phenyl-d_5)-diazene (**3a-*d*$_5$**) was subjected to the standard reaction conditions. After purification by column chromatography and analysis of the ^{1}H NMR spectra and HRMS, a mixture of four products with the same polarity was observed: 5,6-dihydroindazolo[2,3-*a*]quinolines **3a-*d*$_4$** and **3a-*d*$_5$**, and indazolo[2,3-*a*]quinolines **4a-*d*$_4$** and **4a-*d*$_5$** (Fig. 4c). This result suggests the possibility of simultaneous intramolecular and intermolecular hydrogen migrations from the aromatic ring to position 6 of **3a**. Due to the overlapping signals in the ^{1}H NMR and the inability to separate the products by column chromatography, the ratio of the products could not be determined. However, HPLC analysis provided approximate relative concentrations of each compound, with

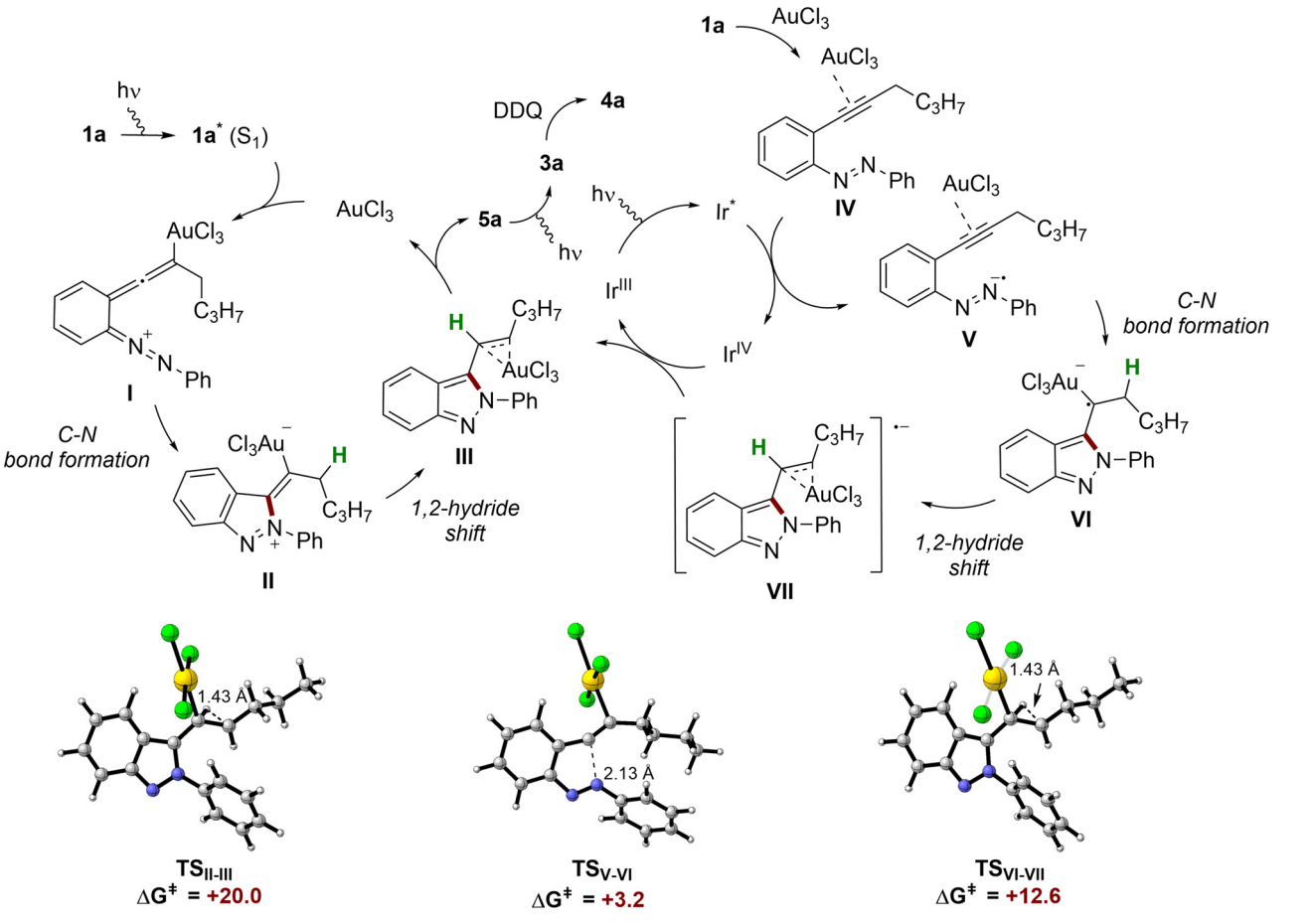

Fig. 5 Mechanistic proposal and DFT calculations. All calculations were conducted at M06/6-311g(d,p)/IEFPCM (solvent = MeCN)/Au (SDD) level of theory (see ESI† for full details). The energy values are given in kcal mol^{-1}.

4a-d_4 being the major product and **3a-d_4** and **3a-d_5** as the minor ones, each with almost the same relative ratio.[38]

Based on the control experiments, it seems that two mechanisms are operating in the formation of indazolo[2,3-*a*]quinolines **4**. DFT calculations were conducted to further investigate the proposed mechanism. A plausible mechanistic hypothesis has been proposed to rationalize the dual gold photoredox catalyzed transformation of 2-alkynylazobenzenes **1** into indazolo[2,3-*a*]quinolines **4**. This hypothesis suggests an initial excitation of **1a** generating the first singlet which by coordination of $AuCl_3$ to the alkynyl moiety, generating intermediate **I**. Next, the formation of a C–N bond (TS not found) generates the indazole intermediate **II**. Next, a 1,2-hydride shift occurs, generating intermediate **III**, with a transition state of $\Delta G^{\ddagger}$ = +20 kcal·mol^{-1}.[42] The elimination of $AuCl_3$ produces 3-alkenyl-2*H*-indazole **5a**, which can cyclize to **3a** in the presence of light. Finally, DDQ facilitates the oxidation of **3a**, yielding the desired indazolo[2,3-*a*]quinoline **4a**. A secondary mechanism involving the Ir(III) catalyst may start with the coordination of $AuCl_3$ to the alkynyl moiety, followed by a single-electron transfer (SET) from the Ir(III) catalyst to intermediate **IV**. This forms radical anion **V** and oxidizes Ir(III) to Ir(IV). Radical anion **V** can then react with the triple bond, forming the C–N bond and giving rise to radical intermediate **VI** through a low-barrier transition state ($\Delta G^{\ddagger}$ = +3.2 kcal mol^{-1}). A 1,2-hydride shift with a transition state energy of +12.6 kcal mol^{-1} delivers intermediate **VII**. This intermediate undergoes a SET process with the Ir(IV) catalyst, oxidizing to intermediate **III** and reducing the iridium catalyst, thus closing the photocatalytic cycle. Intermediate **III** can then evolve to **5a**, closing the gold catalytic cycle (Fig. 5).

Conclusions

In conclusion, this study demonstrates the efficacy of a novel regiodivergent cyclization procedure for transforming 2-alkynylazobenzenes into two distinct azapolyaromatic regioisomers. By manipulating the presence or absence of a gold catalyst and utilizing visible light irradiation, we achieved selective synthesis of 11*H*-indolo[1,2-*b*]indazoles and indazolo[2,3-*a*]quinolines. The mechanistic insights provided by control experiments and DFT calculations reveal that these transformations proceed through different pathways, with radical and polar mechanisms being predominant. This methodology not only enhances the structural diversity of azapolyaromatic compounds but also offers a more sustainable and efficient approach for the discovery and synthesis of new molecules.

Author contributions

Conceptualization: E. M.; methodology: C. M. and E. M.; funding acquisition: E. M.; investigation: C. M., B. I. and E. M.; supervision: E. M.; writing-original draft: E. M.; writing: review & editing: C. M. and E. M.

Data availability

Data for this article, including procedures, NMR spectra description, NMR spectra and DFT results are available at the ESI.†

Conflicts of interest

There are no conflicts to declare.

Note added after first publication

This article replaces the version published on the 28th of October 2024. The structure of Compound A was omitted below Table 1, and the reaction scheme shown at the top of Table 2 was included instead in error. The RSC apologises for any confusion.

Acknowledgements

Financial support was provided by Comunidad de Madrid Research Talent Attraction Program (grant ref. 2018-T1/IND-10054 and 2022-5A/IND-24227), the Spanish Ministry of Science and Innovation (MICINN) (grant ref. CNS2022-135304 and TED2021-129634B-I00) and Universidad de Alcalá (grant ref. CCG20/CC-009 and IUAH21/CC-003). Computational resources for the DFT calculations were provided by the HERMES Cluster at the University of Zaragoza. We also gratefully acknowledge the computing time granted by the Spanish Supercomputing Network (grant ref. QH-2023-2-0005) and provided on CESGA (Galicia Supercomputing Center).

References

1 (*a*) W. Jiang, Y. Li and Z. Wang, Heteroarenes as high-performance organic semiconductors, *Chem. Soc. Rev.*, 2013, **42**, 6113–6127, DOI: **10.1039/c3cs60108k**; (*b*) Z. Chen, W. Li, M. A. Sabuj, Y. Li, W. Zhu, M. Zeng, C. S. Sarap, M. M. Huda, X. Qiao, X. Peng, D. Ma, Y. Ma, N. Rai and F. Huang, Evolution of the electronic structure in open-shell donor-acceptor organic semiconductors, *Nat. Commun.*, 2021, **12**, 5889, DOI: **10.1038/s41467-021-26173-3**.

2 (*a*) N. Benson, O. Suleiman, S. O. Odoh and Z. R. Woydziak, Pyrazole, imidazole, and isoindolone dipyrrinone analogues: pH-dependent fluorophores that red-shift emission frequencies in a basic solution, *J. Org. Chem.*, 2019, **84**, 11856–11862, DOI: **10.1021/acs.joc.9b01708**; (*b*) G. Li, M. Zhao, J. Xie, Y. Yao, L. Mou, X. Zhang, X. Guo, W. Sun, Z. Wang, J. Xu, J. Xue, T. Hu, M. Zhang, M. Li and L. Hong, Efficient synthesis of cyclic amidine-based fluorophores via 6π-electrocyclic ring closure, *Chem. Sci.*, 2020, **11**, 3586–3591, DOI: **10.1039/d0sc00798f**.

3 (*a*) Y. Yang, Y. Wang, Y. Xie, T. Xiong, Z. Yuan, Y. Zhang, S. Qian and Y. Xiao, Fused perylenebisimide–carbazole: new ladder chromophores with enhanced third-order nonlinear optical activities, *Chem. Commun.*, 2011, **47**, 10749–10751, DOI: 10.1039/c1cc14071j; (*b*) M. Stępień, E. Gońka, M. ZÌyła and N. Sprutta, Heterocyclic nanographenes and other polycyclic heteroaromatic compounds: synthetic routes, properties, and applications, *Chem. Rev.*, 2017, **117**, 3479–3716, DOI: 10.1021/acs.chemrev.6b00076; (*c*) Z. Huang, Z. Bin, R. Su, F. Yang, J. Lan and J. You, Molecular design of non-doped OLEDs based on a twisted heptagonal acceptor: a delicate balance between rigidity and rotatability, *Angew. Chem., Int. Ed.*, 2020, **59**, 9992–9996, DOI: 10.1002/anie.201915397.

4 (*a*) J. Akhtar, A. A. Khan, Z. Ali, R. Haider and M. S. Yar, Structure-activity relationship (SAR) study and design strategies of nitrogen-containing heterocyclic moieties for their anticancer activities, *Eur. J. Med. Chem.*, 2017, **125**, 143–189, DOI: 10.1016/j.ejmech.2016.09.023; (*b*) M. M. Heravi and V. Zadsirjan, Prescribed drugs containing nitrogen heterocycles: an overview, *RSC Adv.*, 2020, **10**, 44247–44311, DOI: 10.1039/d0ra09198g.

5 K. Umemura, T. Mizushima, H. Katayama, Y. Kiryu, T. Yamori and T. Andoh, Inhibition of DNA topoisomerases II and/or I by pyrazolo[1,5-*a*]indole derivatives and their growth inhibitory activities, *Mol. Pharmacol.*, 2002, **62**, 873–880, DOI: 10.1124/mol.62.4.873.

6 (*a*) P. Stoessel, H. Heil, D. Joosten, C. Pflumm, A. Gerhard and E. Breuning, Organic electroluminescent materials and devices, WO2010086089A1, 2010 (International patent application); (*b*) P. Stoessel, D. Joosten, A. Gerhard and E. Breuning, Metal Complexes, WO2012007086A1, 2012 (International patent application); (*c*) S.-J. Jung, K.-Y. Kim, J.-M. Hong, S.-J. Eum, J.-D. Lee, J.-H. Jung, M.-J. Kim, Y.-S. No and S.-S. Chung, Polycyclic compound containing pyrazole and organic light-emitting device using same, WO2015034140A1, 2015 (International patent application).

7 M. Vijay, S. V. Kumar, V. Satheesh, P. Ananthappan, H. K. Srivastava, S. Ellairaja, V. S. Vasantha and T. Punniyamurthy, Stereospecific assembly of fused imidazolidines via tandem ring opening/oxidative amination of aziridines with cyclic secondary amines using photoredox catalysis, *Org. Lett.*, 2019, **21**, 7649–7654, DOI: 10.1021/acs.orglett.9b02957.

8 J. P. Michael, Quinoline, quinazoline and acridone alkaloids, *Nat. Prod. Rep.*, 2007, **24**, 223–246, DOI: 10.1039/b509528j.

9 A. Weyesaa and E. Mulugeta, Recent advances in the synthesis of biologically and pharmaceutically active quinoline and its analogues: a review, *RSC Adv.*, 2020, **10**, 20784–20793, DOI: 10.1039/d0ra03763j.

10 (*a*) S. M. Prajapati, K. D. Patel, R. H. Vekariya, S. N. Panchala and H. D. Patel, Recent advances in the synthesis of quinolines: a review, *RSC Adv.*, 2014, **4**, 24463–24476, DOI: 10.1039/c4ra01814a; (*b*) V. F. Batista, D. C. G. A. Pinto and A. M. S. Silva, Synthesis of quinolines: a green perspective, *ACS Sustainable Chem. Eng.*, 2016, **4**, 4064–4078, DOI: 10.1021/acssuschemeng.6b01010.

11 D. J. Gale and J. F. K. Wilshire, Studies in the indazole series. Ring opening of some 1-Arylindazole-3-carboxylic acids during decarboxylation, *Aust. J. Chem.*, 1973, **26**, 2683–2695, DOI: 10.1071/ch9732683.

12 J. Rosevear and J. F. K. Wilshire, Cyclization reactions in azole chemistry: the reaction of some azoles with *o*-fluoroacetophenone, *o*-fluorobenzaldehyde and *o*-fluorobenzophenone, *Aust. J. Chem.*, 1991, **44**, 1097–1114, DOI: 10.1071/ch9911097.

13 (*a*) Y. Zhu, Y. Kiryu and H. Katayama, Intramolecular aromatic amination by a hydrazino group for the synthesis of indolo[1,2-*b*]indazole derivatives, *Tetrahedron Lett.*, 2002, **43**, 3577–3580, DOI: 10.1016/s0040-4039(02)00545-2; (*b*) J. Chi, C. Hang, Y. Zhu and H. Katayama, Synthesis of indolo[1,2-*b*]indazole derivatives via copper(I)-catalyzed intramolecular amination reaction, *Synth. Commun.*, 2010, **40**, 1123–1133, DOI: 10.1080/00397910903043017.

14 C. Guo, B. Li, H. Liu, X. Zhang, X. Zhang and X. Fan, Synthesis of fused or spiro polyheterocyclic compounds via the dehydrogenative annulation reactions of 2-arylindazoles with maleimides, *Org. Lett.*, 2019, **21**, 7189–7193, DOI: 10.1021/acs.orglett.9b01889.

15 H. Zhang, S.-S. Di, X.-B. Huang, Y.-B. Zhou, M.-C. Liu and H.-Y. Wu, Direct dilithiation of N-aryl heterocycles for the construction of condensed N-heterocycles, *Org. Chem. Front.*, 2022, **9**, 2659–2663, DOI: 10.1039/d1qo01896e.

16 (*a*) K. T. Potts, H. P. Youzwak and S. J. Zurawel, Nonclassical heterocycles. 6. Tri- and tetracyclic ring systems containing a "nonclassical" thiophene nucleus, *J. Org. Chem.*, 1980, **45**, 90–97, DOI: 10.1021/jo01289a019; (*b*) Y. Yoshiro, H. Takashi and M. Mitsuo, Reactions of substituted pyridinium N-imines with benzyne: syntheses of pyrido[1,2-*b*]indazoles and related compounds, *Chem. Lett.*, 1980, **9**, 1133–1136, DOI: 10.1246/cl.1980.1133.

17 N. Shindoh, H. Tokuyama, Y. Takemoto and K. Takasu, Auto-tandem catalysis in the synthesis of substituted quinolines from aldimines and electron-rich olefins: cascade Povarov–hydrogen-transfer reaction, *J. Org. Chem.*, 2008, **73**, 7451–7456, DOI: 10.1021/jo8009243.

18 (*a*) J. Zhao, P. Li, C. Wu, H. Chen, W. Ai, R. Sun, H. Ren, R. C. Larock and F. Shi, Aryne [3 + 2] cycloaddition with *N*-sulfonylpyridinium imides and in situ generated N-sulfonylisoquinolinium imides: a potential route to pyrido[1,2-*b*]indazoles and indazolo[3,2-*a*]isoquinolines, *Org. Biomol. Chem.*, 2012, **10**, 1922–1930, DOI: 10.1039/c2ob06611d; (*b*) L. Li, H. Wang, X. Yang, L. Kong, F. Wang and X. Li, Rhodium-catalyzed oxidative synthesis of quinoline-fused sydnones via 2-fold C–H bond activation, *J. Org. Chem.*, 2016, **81**, 12038–12045, DOI: 10.1021/acs.joc.6b02356.

19 B. Haag, Z. Peng and P. Knochel, Preparation of polyfunctional indazoles and heteroarylazo compounds using highly functionalized zinc reagents, *Org. Lett.*, 2009, **11**, 4270–4273, DOI: 10.1021/ol901585k.

20 S. V. Kumar, S. Ellairaja, V. Satheesh, V. S. Vasantha and T. Punniyamurthy, Rh-catalyzed regioselective C–H acti-

vation and C–C bond formation: synthesis and photophysical studies of indazolo[2,3-*a*]quinolines, *Org. Chem. Front.*, 2018, **5**, 2630–2635, DOI: **10.1039/c8qo00557e**.

21 S. Guo, L. Sun, X. Li, X. Zhang and X. Fan, Selective synthesis of indazolo[2,3-*a*]quinolines via Rh(III)-catalyzed oxidant-free [4 + 2] or [5 + 1] annulation of 2-aryl-2*H*-indazoles with α-diazo carbonyl compounds, *Adv. Synth. Catal.*, 2020, **362**, 913–926, DOI: **10.1002/adsc.201901422**.

22 Y. C. Devulapally, C. Ittamalla, S. Balasubramanian and B. V. S. Reddy, Rhodium(III)-catalyzed dehydrogenative annulation of 2-arylindazoles with cyclic enones, *Eur. J. Org. Chem.*, 2021, 3083–3090, DOI: **10.1002/ejoc.202100272**.

23 A. Chidrawar, Y. C. Devulapally, S. Balasubramanian and B. V. S. Reddy, Rh(III)-catalyzed oxidative annulation of 2-arylindazoles with β-ketosulfoxonium ylides, *ChemistrySelect*, 2021, **6**, 13046–13050, DOI: **10.1002/slct.202102982**.

24 W. Hu, C. Pi, D. Hu, X. Han, Y. Wu and X. Cui, Rh(III)-catalyzed synthesis of indazolo[2,3-*a*]quinolines: vinylene carbonate as C1 and C2 building blocks, *Org. Lett.*, 2022, **24**, 2613–2618, DOI: **10.1021/acs.orglett.2c00580**.

25 K. Ghosh, Y. Nishii and M. Miura, Oxidative C-H/C-H annulation of imidazopyridines and indazoles through rhodium-catalyzed vinylene transfer, *Org. Lett.*, 2020, **22**, 3547–3550, DOI: **10.1021/acs.orglett.0c00975**.

26 A. R. Hajipour, Z. Khorsandi and S. Bahri, An efficient and inexpensive visible light photoredox copper catalyst for N-N bond-forming reactions: the one-pot synthesis of indazolo [2,3-*α*]quinolines, *J. Iran. Chem. Soc.*, 2018, **15**, 981–986, DOI: **10.1007/s13738-018-1295-1**.

27 W.-C. Lin and D.-Y. Yang, Visible light photoredox catalysis: synthesis of indazolo[2,3-*a*]quinolines from 2-(2-nitrophenyl)-1,2,3,4-tetrahydroquinolines, *Org. Lett.*, 2013, **15**, 4862–4865, DOI: **10.1021/ol402286d**.

28 (*a*) P. F. Gordon and P. Gregory, *Organic chemistry in colour*, Springer, NY, 1983; (*b*) H. Zollinger, *Color chemistry: syntheses, properties and applications of organic dyes and pigments*, VCH, NY, 1987; (*c*) K. Hunger, *Industrial dyes: chemistry, properties, applications*, ed. Wiley-VCH, Germany, 2003.

29 (*a*) T. Ikeda and O. Tsutsumi, Optical switching and image storage by means of azobenzene liquid-crystal films, *Science*, 1995, **268**, 1873–1875, DOI: **10.1126/science.268.5219.1873**; (*b*) H. Murakami, A. Kawabuchi, K. Kotoo, M. Kutinake and N. Nakashima, A light-driven molecular shuttle based on a rotaxane, *J. Am. Chem. Soc.*, 1997, **119**, 7605–7606, DOI: **10.1021/ja971438a**; (*c*) J. C. Crano and R. Guglielmetti, *Organic Photochromic and Thermochromic Compounds*, Plenum Press, NY, 1999. DOI: **10.1007/b114211**; (*d*) W. Zhen, H. Han, M. Anguiano, C. Lemere, C.-G. Cho and P. T. Lansbury, Synthesis and amyloid binding properties of rhenium complexes: preliminary progress toward a reagent for SPECT imaging of Alzheimer's disease brain, *J. Med. Chem.*, 1999, **42**, 2805–2815, DOI: **10.1021/jm990103w**; (*e*) B. L. Feringa, R. A. Van Delden, N. Koumura and E. M. Geertsema, Chiroptical Molecular Switches, *Chem. Rev.*, 2000, **100**, 1789–1816, DOI: **10.1021/cr9900228**; (*f*) H. Finkelmann, E. Nishikawa, G. G. Pereira and M. Warner, A new opto-mechanical effect in solids, *Phys. Rev. Lett.*, 2001, **87**, 015501, DOI: **10.1103/physrevlett.87.015501**; (*g*) T. Hugel, N. B. Holland, A. Cattani, L. Moroder, M. Seitz and H. E. Gaub, Single-molecule optomechanical cycle, *Science*, 2002, **296**, 1103–1106, DOI: **10.1126/science.1069856**; (*h*) I. A. Banerjee, L. Yu and H. Matsui, Application of host-guest chemistry in nanotube-based device fabrication: photochemically controlled immobilization of azobenzene nanotubes on patterned α-CD monolayer/Au substrates via molecular recognition, *J. Am. Chem. Soc.*, 2003, **125**, 9542–9543, DOI: **10.1021/ja0344011**; (*i*) A. Jain, Y. Gupta and S. K. Jain, Azo chemistry and its potential for colonic delivery, *Crit. Rev. Ther. Drug Carrier Syst.*, 2006, **23**, 349–400, DOI: **10.1615/critrevtherdrugcarriersyst.v23.i5.10**; (*j*) *Smart light-responsive materials*, ed. Y. Zhao and T. Ikeda, John Wiley & Sons, Hoboken, NJ, 2009; (*k*) *Molecular switches*, ed. B. L. Feringa and W. R. Browne, Wiley-VCH, 2011; (*l*) A. Polosukhina, J. Litt, I. Tochitsky, J. Nemargut, Y. Sychev, I. De Kouchkovsky, T. Huang, K. Borges, D. Trauner, R. N. Van Gelder and R. H. Kramer, Photochemical restoration of visual responses in blind mice, *Neuron*, 2012, **75**, 271–282, DOI: **10.1016/j.neuron.2012.05.022**; (*m*) W. A. Velema, W. Szymanski and B. L. Feringa, Photopharmacology: beyond proof of principle, *J. Am. Chem. Soc.*, 2014, **136**, 2178–2191, DOI: **10.1021/ja413063e**; (*n*) J. Zhu, T. Guo, Z. Wang and Y. Zhao, Triggered azobenzene-based prodrugs and drug delivery systems, *J. Controlled Release*, 2022, **345**, 475–493, DOI: **10.1016/j.jconrel.2022.03.041**; (*o*) C. Fedele, T. P. Ruoko, K. Kuntze, M. Virkki and A. Priimagi, New tricks and emerging applications from contemporary azobenzene research, *Photochem. Photobiol. Sci.*, 2022, **21**, 1719–1734, DOI: **10.1007/s43630-022-00262-8**.

30 (*a*) N. Siampiringue, G. Guyot, S. Monti and P. Bortolus, The *cis* → *trans* photoisomerization of azobenzene: an experimental re-examination, *J. Photochem.*, 1987, **37**, 185–188, DOI: **10.1016/0047-2670(87)85039-6**; (*b*) A. Cembran, F. Bernardi, M. Garavelli, L. Gagliardi and G. Orlandi, On the mechanism of the *cis–trans* isomerization in the lowest electronic states of azobenzene: S0, S1, and T1, *J. Am. Chem. Soc.*, 2004, **26**, 3234–3243, DOI: **10.1021/ja038327y**; (*c*) E. Merino and M. Ribagorda, Control over molecular motion using the *cis–trans* photoisomerization of the azo group, *Beilstein J. Org. Chem.*, 2012, **8**, 1071–1090, DOI: **10.3762/bjoc.8.119**; (*d*) M. Quick, A. L. Dobryakov, M. Gerecke, C. Richter, F. Berndt, I. N. Ioffe, A. A. Granovsky, R. Mahrwald, N. P. Ernsting and S. A. Kovalenko, Photoisomerization dynamics and pathways of *trans*- and *cis*-azobenzene in solution from broadband femtosecond spectroscopies and calculations, *J. Phys. Chem. B*, 2014, **118**, 8756–8771, DOI: **10.1021/jp504999f**; (*e*) I. C. D. Merritt, D. Jacquemin and M. Vacher, *Cis-trans*

photoisomerisation of azobenzene: a fresh theoretical look, *Phys. Chem. Chem. Phys.*, 2021, **23**, 19155–19165, DOI: 10.1039/d1cp01873f.

31 (*a*) A. M. Sánchez and R. H. de Rossi, Solvent effects on the thermal *cis-trans* isomerization and charge-transfer absorption of 4-(diethylamino)-4′-nitroazobenzene, *J. Org. Chem.*, 1996, **61**, 3446–3451, DOI: 10.1021/jo00165a005; (*b*) M. Alemani, M. V. Peters, S. Hecht, K.-H. Rieder, F. Moresco and L. Grill, Electric field-induced isomerization of azobenzene by STM, *J. Am. Chem. Soc.*, 2006, **128**, 14446–14447, DOI: 10.1021/ja065449s; (*c*) G. L. Hallett-Tapley, C. D'Alfonso, N. L. Pacioni, C. D. McTiernan, M. González-Béjar, O. Lanzalunga, E. I. Alarcona and J. C. Scaiano, Gold nanoparticle catalysis of the *cis–trans* isomerization of azobenzene, *Chem. Commun.*, 2013, **49**, 10073–10075, DOI: 10.1039/c3cc41669k; (*d*) S. K. Surampudi, H. R. Patel, G. Nagarjunaa and D. Venkataraman, Mechano-isomerization of azobenzene, *Chem. Commun.*, 2013, **49**, 7519–7521, DOI: 10.1039/c3cc43797c; (*e*) A. Goulet-Hanssens, M. Utecht, D. Mutruc, E. Titov, J. Schwar, L. Grubert, D. Bléger, P. Saalfrank and S. Hecht, Electrocatalytic $Z \rightarrow E$ isomerization of azobenzenes, *J. Am. Chem. Soc.*, 2017, **139**, 335–341, DOI: 10.1021/jacs.6b10822.

32 (*a*) G. E. Lewis and R. J. Mayfield, Photoinduced reaction of azobenzene with acetyl chloride, *Tetrahedron Lett.*, 1966, **7**, 269–271, DOI: 10.1016/s0040-4039(00)70226-7; (*b*) X. Ke, S. Sarina, J. Zhao, X. Zhang, J. Changa and H. Zhu, Tuning the reduction power of supported gold nanoparticle photocatalysts for selective reductions by manipulating the wavelength of visible light irradiation, *Chem. Commun.*, 2012, **48**, 3509–3511, DOI: 10.1039/c2cc17977f; (*c*) F. Cumine, F. Palumbo and J. A. Murphy, Reduction of nitroarenes, azoarenes and hydrazine derivatives by an organic super electron donor, *Tetrahedron*, 2018, **74**, 5539–5545, DOI: 10.1016/j.tet.2018.04.069; (*d*) N. Xu, Y. Zhang, W. Chen, P. Li and L. Wang, Photoinduced N-methylation and N-sulfonylation of azobenzenes with DMSO under mild reaction conditions, *Adv. Synth. Catal.*, 2018, **360**, 1199–1208, DOI: 10.1002/adsc.201701548; (*e*) X. Wang, X. Wang, C. Xia and L. Wu, Visible-light-promoted oxidative dehydrogenation of hydrazobenzenes and transfer hydrogenation of azobenzenes, *Green Chem.*, 2019, **21**, 4189–4193, DOI: 10.1039/c9gc01618j; (*f*) Y. Katsuma, L. Wu, Z. Lin, S. Akiyama and M. Yamashita, Reactivity of a tetra(*o*-tolyl) diborane(4) dianion as a diarylboryl anion equivalent, *Angew. Chem., Int. Ed.*, 2019, **58**, 317–321, DOI: 10.1002/anie.201907400; (*g*) J. Yang, M. Song, H. Zhou, G. Wang, B. Ma, Y. Qi and C. Huo, Visible-light-mediated hydroacylation of azobenzenes with α-keto acids, *Org. Lett.*, 2020, **22**, 8407–8412, DOI: 10.1021/acs.orglett.0c03039; (*h*) M. Song, H. Zhou, G. Wang, B. Ma, Y. Jiang, J. Yang, C. Huo and X.-C. Wang, Visible-light-promoted diboron-mediated transfer hydrogenation of azobenzenes to hydrazobenzenes, *J. Org. Chem.*, 2021, **86**, 4804–4811, DOI: 10.1021/acs.joc.1c00394; (*i*) J. Yang, M. Song, H. Zhou, Y. Qi, B. Ma and X.-C. Wang, Visible-light-promoted decarboxylative addition cyclization of N-aryl glycines and azobenzenes to access 1,2,4-triazolidines, *Green Chem.*, 2021, **23**, 5806–5811, DOI: 10.1039/d1gc02272e; (*j*) J. Yang, C. Wang, H. Zhou, Q. Kong and W. Ma, Visible-light-driven hydrophosphorylation of azobenzenes enabled by *trans*-to-*cis* photoisomerization, *Adv. Synth. Catal.*, 2022, **364**, 4275–4280, DOI: 10.1002/adsc.202201089; (*k*) Q. Li, Y. Luo, J. Chen and Y. Xia, Visible-light-promoted hydrogenation of azobenzenes to hydrazobenzenes with thioacetic acid as the reductant, *J. Org. Chem.*, 2023, **88**, 2443–2452, DOI: 10.1021/acs.joc.2c02873; (*l*) J. Yang, C. Wang, B. Huang, H. Zhou, J. Li and X. Liu, Photoredox catalytic phosphine-mediated deoxygenative hydroacylation of azobenzenes with carboxylic acids, *Org. Lett.*, 2024, **26**, 498–502, DOI: 10.1021/acs.orglett.3c03875.

33 V. A. K. Adiraju and C. D. Martin, Isomer dependence on the reactivity of diazenes with pentaphenylborole, *Chem. – Eur. J.*, 2017, **23**, 11437–11444, DOI: 10.1002/chem.201702539.

34 W. Zhang, J. Bu, L. Wang, P. Li and H. Li, Sunlight-mediated [3 + 2] cycloaddition of azobenzenes with arynes: an approach toward the carbazole skeleton, *Org. Chem. Front.*, 2021, **8**, 5045–5051, DOI: 10.1039/d1qo00739d.

35 C. Mañas and E. Merino, Visible light-mediated heterodifunctionalization of alkynylazobenzenes for 2*H*–indazole synthesis, *Org. Lett.*, 2024, **26**, 1868–1873, DOI: 10.1021/acs.orglett.4c00097.

36 (*a*) B. E. Moulton, H. Dong, C. T. O'Brien, S. B. Duckett, Z. Lin and I. J. S. Fairlamb, A natural light induced regioselective 6π-electrocyclisation–oxidative aromatisation reaction: experimental and theoretical insights, *Org. Biomol. Chem.*, 2008, **6**, 4523–4532, DOI: 10.1039/b811284c; (*b*) J. Xi, D. Wang, J. Hu, H. Shen, T. Wang and Z. Zhang, Rearrangement of 2-(benzofuran-2-yl)-3-phenylpyridines via photoinduced 6π-electrocyclization, *Org. Biomol. Chem.*, 2023, **21**, 7188–7193, DOI: 10.1039/d3ob00883e.

37 Deposition numbers CCDC 2374941 (for **2s**), by 2374943 (for **3j**) and 2374942 (for **4b**) contain the supporting crystallographic data for this paper.†

38 For more details, see ESI.†

39 (*a*) S. Kato, Y. Saga, M. Kojima, H. Fuse, S. Matsunaga, A. Fukatsu, M. Kondo, S. Masaoka and M. Kanai, Hybrid catalysis enabling room-temperature hydrogen gas release from N-heterocycles and tetrahydronaphthalenes, *J. Am. Chem. Soc.*, 2017, **139**, 2204–2207, DOI: 10.1021/jacs.7b00253; (*b*) K.-H. He, F.-F. Tan, C.-Z. Zhou, G.-J. Zhou, X.-L. Yang and Y. Li, Acceptorless dehydrogenation of N-heterocycles by merging visible-light photoredox catalysis and cobalt catalysis, *Angew. Chem., Int. Ed.*, 2017, **56**, 3080–3084, DOI: 10.1002/ange.201612486; (*c*) J. Fan, W. Zhang, W. Gao, T. Wang, W.-L. Duan, Y. Liang and Z. Zhang, Syntheses of benzofuranoquinolines and analogues via photoinduced acceptorless dehydrogenative annulation of *o*-phenylfuranylpyridines, *Org. Lett.*, 2019, **21**, 9183–9187, DOI: 10.1021/acs.orglett.9b03556; (*d*) Y. Kang, W. Zhang, T. Wang, Y. Liang and Z. Zhang, Two-step synthesis of π-expanded maleimides from 3,4-diphenylfuran-2(5*H*)-

ones, *J. Org. Chem.*, 2019, **84**, 12387–12398, DOI: **10.1021/acs.joc.9b01792**; (*e*) M.-J. Zhou, L. Zhang, G. Liu, C. Xu and Z. Huang, Site-selective acceptorless dehydrogenation of aliphatics enabled by organophotoredox/cobalt dual catalysis, *J. Am. Chem. Soc.*, 2021, **143**, 16470–16485, DOI: **10.1021/jacs.1c05479**.

40 Even thought, traces of 5,6-dihydroindazolo[2,3-*a*]quinoline **3x** could be detected by ^{1}H NMR spectroscopy in the crude mixture, the two products could be purified by column chromatography.

41 G. S. Hammond, J. Saltiel, A. A. Lamola, N. J. Turro, J. S. Bradshaw, D. O. Cowan, R. C. Counsell, V. Vogt and C. Dalton, Mechanisms of photochemical reactions in solution. XXII. Photochemical *cis-trans* isomerization, *J. Am. Chem. Soc.*, 1964, **86**, 3197–3217, DOI: **10.1021/ja01070a002**.

42 (*a*) I. V. Seregin and V. Gevorgyan, Gold-Catalyzed 1,2-Migration of Silicon, Tin, and Germanium en Route to C-2 Substituted Fused Pyrrole-Containing Heterocycles, *J. Am. Chem. Soc.*, 2006, **128**, 12050–12051, DOI: **10.1021/ja063278l**; (*b*) I. V. Seregin, A. W. Schammel and V. Gevorgyan, Multisubstituted *N*-fused heterocycles via transition metal-catalyzed cycloisomerization protocols, *Tetrahedron*, 2008, **64**, 6876–6883, DOI: **10.1016/j.tet.2008.04.023**.